J. Ocean Univ. China (Oceanic and Coastal Sea Research)
DOI 10.1007/s11802-011-1813-1
ISSN 1672-5182, 2012 11 (2): 137-146
http://www.ouc.edu.cn/xbywb/
E-mail:xbywb@ouc.edu.cn

Doctor Forum

Spatial-Temporal Variations of Dominant Drought/Flood Modes and the Associated Atmospheric Circulation and Ocean Events in Rainy Season over the East of China

HUANG Shaoni[1), 2)], and HUANG Fei[1), *]

1) *Physical Oceanography Laboratory and Key Laboratory of Ocean-Atmosphere Interaction and Climate in Universities of Shandong*, *Ocean University of China*, *Qingdao* 266100, *P. R. China*
2) *Shanxi Meteorological Observatory*, *Xi'an* 710014, *P. R. China*

(Received December 2, 2010; revised March 21, 2011; accepted September 13, 2011)

Abstract By using Season-reliant Empirical Orthogonal Function (S-EOF) analysis, three dominant modes of the spatial-temporal evolution of the drought/flood patterns in the rainy season over the east of China are revealed for the period of 1960−2004. The first two leading modes occur during the turnabout phase of El Niño-Southern Oscillation (ENSO) decaying year, but the drought/flood patterns in the rainy season over the east of China are different due to the role of the Indian Ocean (IO). The first leading mode appears closely correlated with the ENSO events. In the decaying year of El Niño, the associated western North Pacific (WNP) anticyclone located over the Philippine Sea persists from the previous winter to the next early summer, transports warm and moist air toward the southern Yangtze River in China, and leads to wet conditions over this entire region. Therefore, the precipitation anomaly in summer exhibits a 'Southern Flood and Northern Drought' pattern over East China. On the other hand, the basin-wide Indian Ocean sea surface temperature anomaly (SSTA) plays a crucial role in prolonging the impact of ENSO on the second mode during the ENSO decaying summer. The Indian Ocean basin mode (IOBM) warming persists through summer and unleashes its influence, which forces a Matsuno-Gill pattern in the upper troposphere. Over the subtropical western North Pacific, an anomalous anticyclone forms in the lower troposphere. The southerlies on the northwest flank of this anticyclone increase the moisture transport onto central China, leading to abundant rainfall over the middle and lower reaches of the Yangtze River and Huaihe River valleys. The anomalous anticyclone causes dry conditions over South China and the South China Sea (SCS). The precipitation anomaly in summer exhibits a 'Northern Flood and Southern Drought' pattern over East China. Therefore, besides the ENSO event the IOBM is an important factor to influence the drought/flood patterns in the rainy season over the east of China. The third mode is positively correlated with the tropical SSTA in the Indian Ocean from the spring of preceding year(–1) to the winter of following year(+1), but not related to the ENSO events. The positive SSTA in the South China Sea and the Philippine Sea persists from spring to autumn, leading to weak north-south and land-sea thermal contrasts, which may weaken the intensity of the East Asia summer monsoon. The weakened rainfall over the northern Indian monsoon region may link to the third spatial mode through the 'Silk Road' teleconnection or a part of circumglobal teleconnection (CGT). The physical mechanisms that reveal these linkages remain elusive and invite further investigation.

Key words ENSO; IOBM; S-EOF; drought/flood patterns

1 Introduction

The rainy season in China experiences several obvious stages from spring to autumn, including the spring rainy season south of the Yangtze River (Zhu *et al.*, 1981; Wan and Wu, 2008), the pre-flooding season in South China (Wang and Ding, 2007), the Meiyu in the Yangtze River and the Huaihe River valleys (Tao and Chen, 1987; Ding, 1992; Tanaka, 1992), the rainy season in North and Northeast China (Matsumoto, 1997; Zhao, 1994), the late flooding season in South China, and the autumn rainy season in West China. As the onset and the seasonal northward movement of the East Asian monsoon, the major rain belts occur accordingly from south to north over the east of China. Anomalous rainfalls concentrated in the summer rainy season in China frequently result in floods and droughts. Therefore, many researchers have paid great attention to the climatic characters and variations of flood/drought during this season over the east of China. Most of the study results (Deng *et al.*, 1989; Wei and Li 1995; Wang *et al.*, 1998; Zhao, 1999) show an alternate flood and drought pattern in the summer rainy season over the east of China. The most significant regional feature is the precipitation anomaly over North and South China, the variation of which always appears out of phase with that over the Yangtze and the Huaihe river valleys. However, recent studies have indicated that monthly precipitation anomalies are not concurrent during a summer rainy season (Wang and Wu, 1996; Zhang *et al.*, 2003;

* Corresponding author. E-mail: huangf@ouc.edu.cn

Chen *et al.*, 2007); the flood/drought pattern over the areas concerned even has a sharp change during the rainy season (Wu *et al.*, 2006, 2007). Recently, many researchers have applied the S-EOF (Season-reliant Empirical Orthogonal Function) analysis to the seasonal mean precipitation over East Asia (Wu *et al.*, 2009) and to the Asian-Australian monsoon (Zhou *et al.*, 2009). According to these research findings, it is necessary to depict the major modes of seasonal evolution of rainfall anomaly throughout the rainy season over China, and to examine what processes give rise to the leading mode of variability.

To reveal the behavior of seasonally evolving anomalies, the S-EOF (Wang and An, 2005) has been applied to rainfall data analysis for the rainy season over China (Huang *et al.*, 2009). Three dominant modes were found, the corresponding spatial-temporal characteristics were described, and the possible processes that give rise to the variability of the three leading modes were discussed. The seasonal evolution of drought/flood patterns in the rainy season over China reflects the seasonally evolving patterns of interannual and interdecadal variability of the eastern Asia summer monsoon (EASM). The relationship between the eastern Pacific SSTA and the East Asia monsoon has been the subject of many studies in the last few decades (*e.g.*, Huang and Wu, 1989; Liu and Ding, 1992; Shen and Lau, 1995; Weng *et al.*, 1999; Wang *et al.*, 2000). The El Niño-Southern Oscillation (ENSO) has been regarded as a major factor to modulate the interannual variability of EASM (Huang and Wu, 1989; Chang *et al.*, 2000a, b; Lau and Weng, 2001). The most pronounced low-level anomalous anticyclone over the western North Pacific (WNPAC), persisting from the El Niño mature winter to the subsequent summer, plays a crucial role in the El Niño-EASM teleconnection (Wang *et al.*, 2000; Chang *et al.*, 2000a, b; Zhou *et al.*, 2009). In early summer, WNPAC is primarily supported by the local negative SSTA, whereas in late summer, IOBM plays a more important role in maintaining WNPAC (Wu *et al.*, 2010).

Recently, many studies have found that the basin-wide warming in the Indian Ocean as a response to El Niño (Yang *et al.*, 2007), land-sea thermal difference over East Asia (Sun *et al.*, 2000, 2002), snow cover on the Tibetan Plateau and Eurasia (*e.g.*, Hsu and Liu, 2003; Wu and Kirtman, 2007), and the position abnormalities of the East Asian subtropical westerly jet (Kuang and Zhang, 2006; Yang and Zhang, 2007a, b; Du *et al.*, 2009) have impact on rainfall variability associated with EASM. In this study, the possible processes that give rise to the top three leading modes of the seasonal evolution of rainfall anomaly will be examined and discussed.

The organization of the paper is as follows. Data and analysis tools used in this study are described in Section 2. Section 3 discusses the atmospheric circulation and the SSTA pattern that give rise to the leading modes. A summary is given in Section 4.

2 Data and Methodology

The observed precipitation data were derived from the Climate Prediction (CPC) Merged Analysis of Precipitation (CMAP) for the period of 1979−2004 and used in the regression analysis. The current data were obained from the National Centers for Environmental Prediction-National Center for Atmospheric Research (NCEP-NCAR) reanalysis (Kalnay and Coauthors, 1996) and sea surface temperature (SST) data from the monthly Hadley Center sea ice and SST data set (HadISST) for the 45-year period of 1960−2004. The Niño-3.4 index is defined as the monthly SST averaged over the western Pacific (5˚S−5˚N, 170˚−120˚W). The traditional four consecutive seasonal mean spanning from March-May (MAM) in year 0 [MAM(0)] to December (0)-February [DJF] the following year [year1; D(0)JF(1))], are linked together.

The collection period for daily rainfall data at 436 observational stations in China has been extended from 2000 to 2004. The S-EOF analysis is also applied to this extended data as Huang *et al.* (2009) did. The results show that the spatial patterns (figures not shown) closely resemble those of Huang *et al.* (2009) (their Fig.3). The first three leading modes account for 9.2%, 7.6%, and 6.5% of the total variance, respectively. The seasonal evolution of drought/flood patterns exhibits complicated spatial and temporal structures in the rainy season over China (Wang *et al.*, 1998; Wang and Tu, 2002), Huang *et al.* (2009) made sensitivity tests to choose the significant top three leading modes. The principal components (PCs) (Fig.1) from this study are highly correlated with those of Huang *et al.* (2009), correlation coefficients being 0.98, 0.94, and 0.91 for the first three modes, respectively. In the following analysis, these new PCs（Fig.1）are used to generate the regression fields of the precipitation, atmospheric circulation, and SST patterns associated with the top three modes.

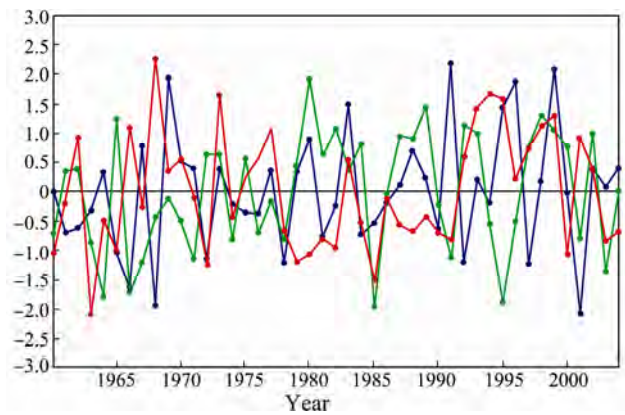

Fig.1 The principal components (PC1, PC2, and PC3) of the first (red line), the second (blue line), and the third (green line) S-EOF modes.

3 Dominant Seasonally Evolving Drought/Flood Patterns

According to seasonal evolution, the rainy seasons are divided into three major periods from spring to autumn. The first period is termed as the pre-peak rainy season from mid-March to mid-May before the EASM onset, the

second period is termed as the peak rainy season from mid-May to mid-July, including the pre-flooding period in South China and the Meiyu or Baiu rainy period in the Yangtze and the Huaihe valleys, and the third period is called the post-peak rainy season from mid-July to mid-September, including the rainy period in the northern and northeastern China and the typhoon rainfall period in South China.

The seasonally evolving drought/flood patterns of the top three modes are shown in Fig.2. Here the precipitation rate anomalies are regressed upon the top three PCs' time series. The precipitation rate anomaly of the first mode (Fig.2a) exhibits a south-north wet-dry seesaw pattern most significantly in the peak rainy season (16 May−15 July), with wet (dry) conditions over the entire area south of the Yangtze River (south of 30˚N) and dry (wet) conditions over the region between the Yellow River and the Yangtze River. This rainfall pattern is similar to the second EOF mode of the summer monsoon rainfall pattern defined by Zhou and Yu (2005) (their Fig.2b), but a heavier rainbelt controls the area between the Yangtze River and the Yellow River valleys and the entire area south of the Yangtze River (south of 30˚N) is dry. These wet (dry) areas over the south of the Yangtze River weaken considerably in the post-peak rainy season, and even dry (wet) areas occur in the southeast coastal region. In the pre-peak rainy season (16 March−15 May), the areas over the north of Yangtze River do not show any obvious precipitation anomaly, while both wet and dry areas occur south of the Yangtze River (Fig.2a).

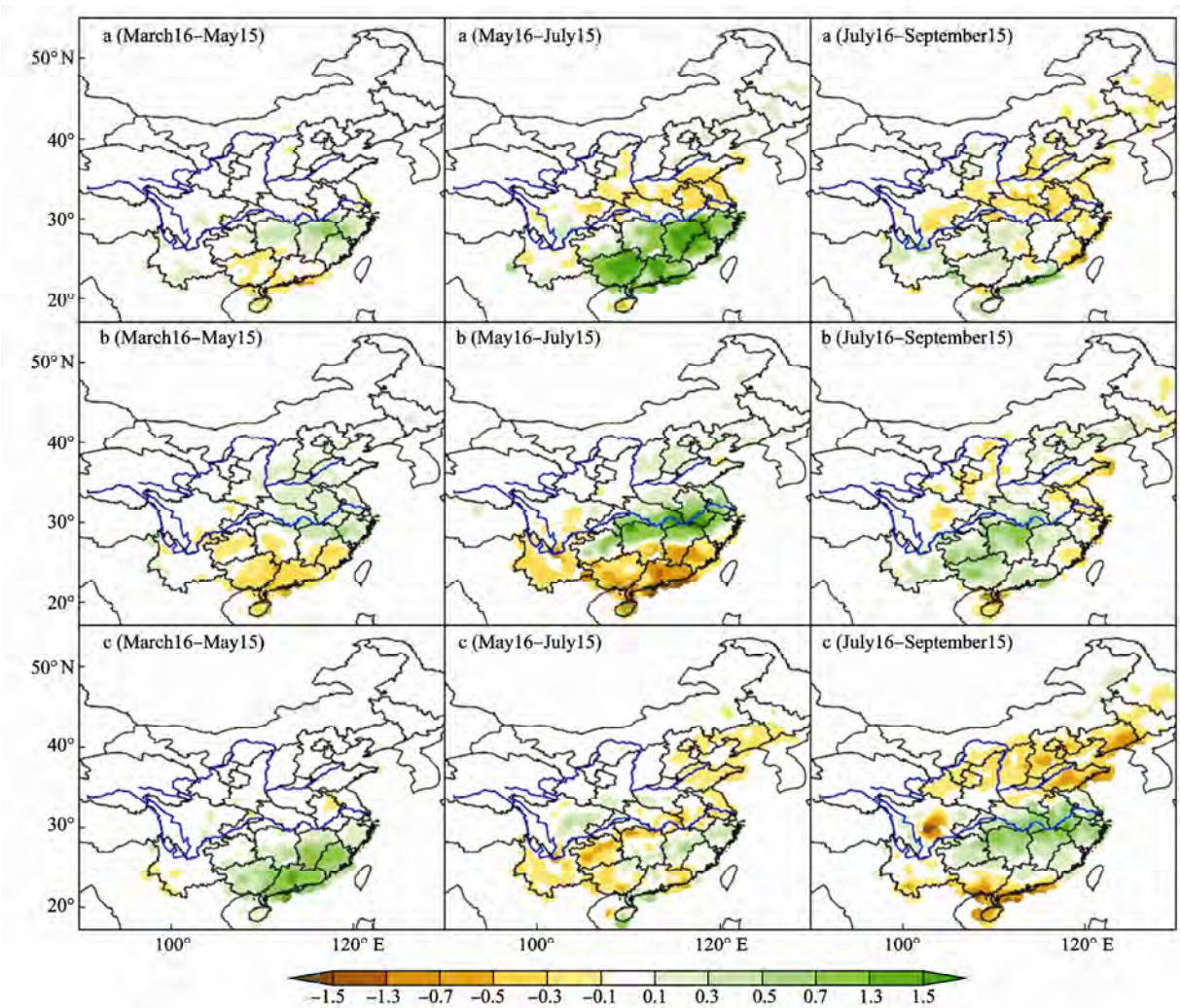

Fig.2 Seasonally evolving patterns of rainfall rate anomalies regressed onto the PCs of the top three S-EOF modes. (a) S-EOF1; (b) S-EOF2; (c) S-EOF3.

The second mode (Fig.2b) also shows a north-south seesaw pattern with wet(dry) areas over the middle and lower reaches of the Yangtze River and the Huaihe River valleys and dry(wet) area over South China from the pre-peak rainy season to the peak rainy season. The most significant rainfall also occurs in the peak rainy season (16 May−15 July), which resembles the typical anomalous rainfall pattern during the summer monsoon with positive anomalies over the middle and lower reaches of the Yangtze River valley (Zhou and Yu, 2005). Compared to the seesaw pattern of the first mode, the zero line of the wet-dry overturn in the second mode shifts southward. During the post-peak rainy season (16 July−15 September), the wet(dry) areas over the middle and lower reaches of the Yangtze River extend southwestward and slightly weaken, while the dry(wet) areas occur in the coastal areas of East

China. It is noticeable that dry conditions in Guangdong, Guangxi, Yunnan, and southern Jiangxi and Hunan provinces during the peak rainy season change to wet conditions in the post-peak season, indicating a drought/flood coexistence and a sudden pattern shift during the summer rainy season (May−September).

The rainfall anomaly of the third mode (Fig.2c) shows a dry(wet)-wet(dry)-dry(wet) wave-train-like pattern from the south to north China in the post-peak rainy season (16 July−15 September). In the pre-peak rainy season (16 March−15 May), the wet(dry) areas control most of the southern Yangtze River region and weaken in the subsequent periods. The dry(wet) areas appear over North China in the peak rainy season, continue to move westward in the post-peak rainy season, and form the northern part of the wave-train-like pattern.

4 Associated Atmospheric Circulation and SST Patterns

4.1 The First Mode

Fig.3 shows the seasonally evolving SSTA, 850-hPa wind anomalies and precipitation rate anomalies associated with the principal component of the first S-EOF (PC1). The seasonal SST evolution in the tropics indicates that the first mode of rainfall anomalies over the east of China in the rainy season occurs during the decaying and turnabout periods of ENSO (Fig.3a). For this analysis further investigation of lead-lag correlations of PC1 with Niño-3.4 index (solid line) and partial lead-lag correlations of PC1 with the area-averaged SSTA over the tropical Indian Ocean (10˚S−10˚N, 40˚E−110˚E) (removing the influence of Niño-3.4 index) shows more evidence for this analysis (Fig.4a). Here year(−1) [year(1)] denotes that Niño-3.4 leads (lags) the PC1 by one year. Fig.4a shows that the first leading mode appears closely correlated with the ENSO events. The PC1 is positively correlated with the summer (JJA) Niño-3.4 index with a correlation coefficient of exceeding 0.25 in year(–1) and above the threshold of the 90% confidence level. This indicates that the first mode occurs in the decaying summer of the ENSO event, with wet(dry) conditions to the south of the Yangtze-river in China from the pre-peak to peak season following the mature phase of El Niño (La Nina). It is noticeable that the mid-latitude SST anomaly in the western North Pacific, including the Japan Sea, the eastern coastal seas of China, and the Korushio extension region, is also closely related to the first mode of the rainfall pattern, and may play an important role in the interdecadal variability of PC1 (Huang *et al.*, 2009).

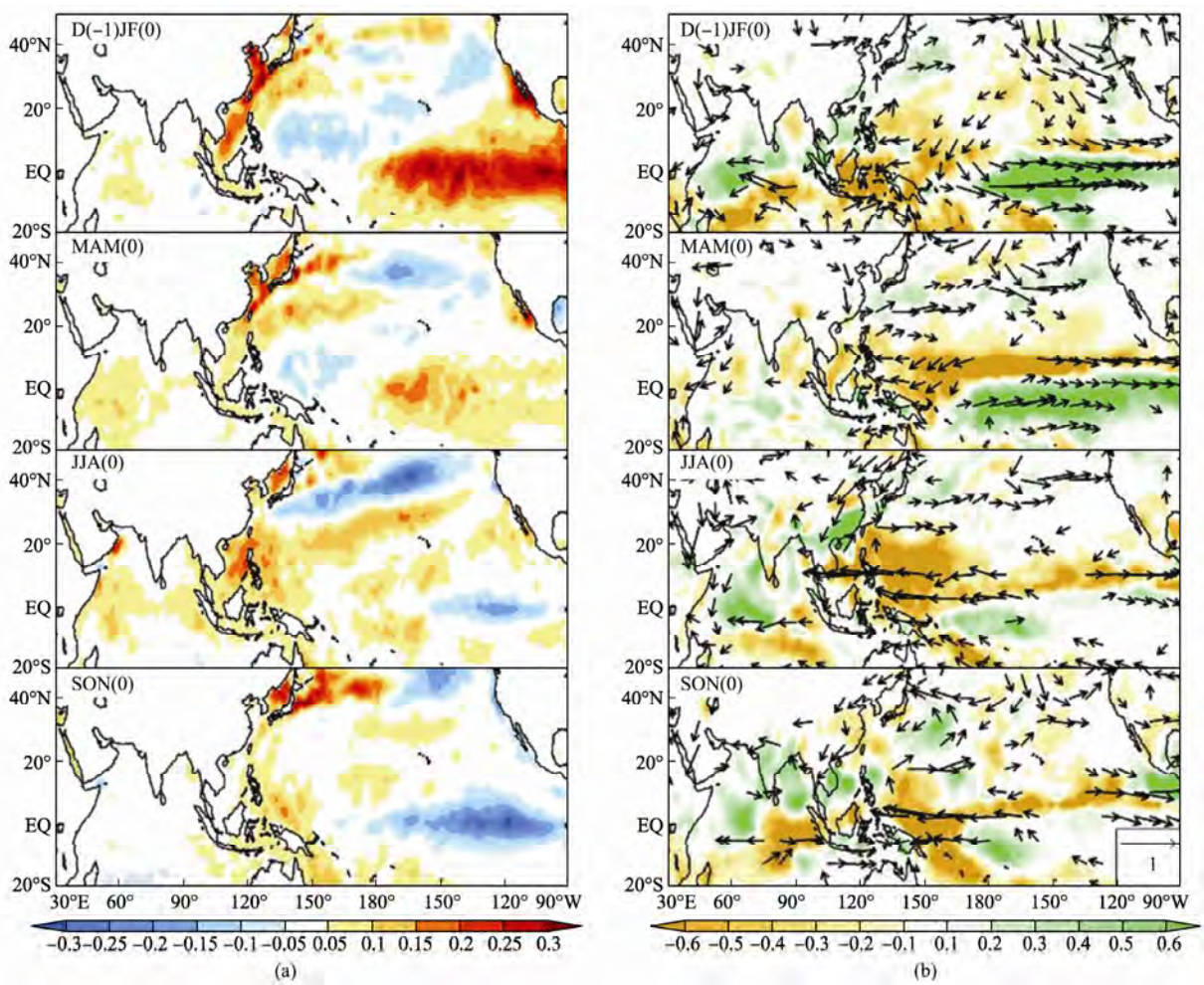

Fig.3 Seasonally evolving patterns of (a) SST (shaded; ℃) anomalies regressed onto the principal component of the first S-EOF; (b) as in (a), but for 850-hPa wind (m s^{-1}; vector) and precipitation rate (shaded; mm d^{-1}).

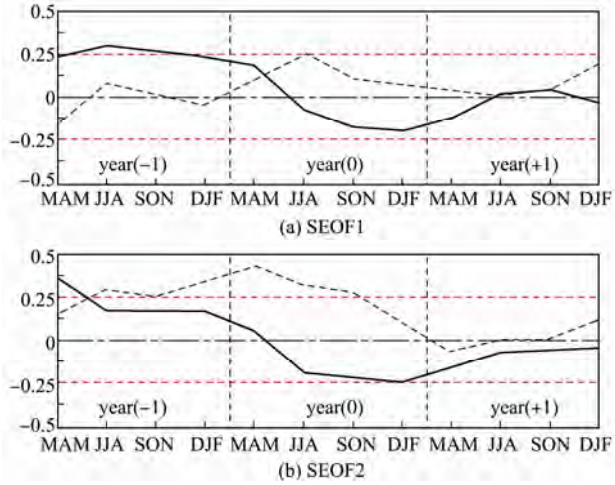

Fig.4 (a) Lead-lag correlations between the first S-EOF principal component and the Niño-3.4 index (solid line), and partial lead-lag correlations between the first S-EOF principal component and the Indian Ocean basin-wide warming index (dashed line). The Indian Ocean basin-wide warming index is defined as the area-averaged SSTA in the tropical Indian Ocean (10°S−10°N, 40°E−110°E). (b) The same as in (a), but for the second mode.

During the El Niño mature phase from December (year −1)–February (year 0) [D(−1)JF(0)], the SSTA is positive in the equatorial central-eastern Pacific, the South China Sea, and the eastern coastal regions of China. Meanwhile, the SSTA is negative over the tropical northwestern Pacific between the Philippines and the international date line, and it weakens somewhat in magnitude but remains negative in the subsequent spring MAM (0) (Fig.3a). Because of the positive thermodynamic air-sea feedback from the local negative SSTA, the western North Pacific (WNP) anticyclone located over the Philippine Sea could sustain from the previous winter to early summer. This anomalous WNP anticyclone causes anomalous wet conditions along the East Asian polar front stretching from South China northeastward to East Japan (Wang *et al.*, 2000).

In the decaying summer of El Niño JJA (0), as the mean flow changes its direction to the southwest over the WNP, the positive air-sea feedback that appears in the preceding winter and spring is no longer valid. Rather, a negative wind-evaporation-SST feedback leads to the decay of the negative SSTA in the WNP (Wang *et al.*, 2000, 2003). Therefore, the positive SSTA over the coastal areas of southeastern China expands to the northwestern tropical Pacific in summer (Fig.3a). Meanwhile, the anomalous southwesterly flows along the northwest flank of the anomalous Philippine Sea anticyclone transport the warm and moist air toward the south of the Yangtze River, and lead to wet conditions over the area (Fig.3b). Thus, the precipitation anomaly in summer exhibits a 'Southern Flood and Northern Drought' pattern over East China.

In SON(0), the negative SSTA strengthens over the equatorial central Pacific (Fig.3a). Meanwhile, the development of a La Nina episode results in the eastward shift of the WNP anomalous anticyclone (Fig.3b).

4.2 The Second Mode

PC2 is positively correlated with the Niño-3.4 index in year(−1), decays rapidly in late winter and the following spring, and reverses the sign in early summer (Fig.4b). The significant negative correlation between PC2 and the Niño-3.4 from summer (JJA(0)) to winter (DJF(0)) in year(0) suggests that the second mode is primarily associated with the turnabout of ENSO. Meanwhile, the significant correlation (larger than 0.4) between PC2 and the tropical IO index from summer JJA in year(−1) to fall SON(0) in year(0) suggests that the basin-wide IO SSTA plays a crucial role in prolonging the impact of ENSO on the second mode during the ENSO decaying summer (Fig.4b). Thus, the first two S-EOF modes reflect seasonally evolving dominant rainfall patterns during the decaying and turnabout year of ENSO, and the basin-wide IO SSTA plays a more significant role in the second mode during the decaying summer of ENSO.

The seasonally evolving atmospheric circulation and SSTA pattern associated with the second mode are shown in Fig.5. Here the 850-hPa wind, precipitation rate, 200-hPa geopotential height (H200 hereafter), and SST anomalies are regressed upon the PC2 time series. It can be seen that the low-frequency ENSO mode accompanies the IOBM during the ENSO mature and decaying phases (Huang *et al.*, 2010), and the second mode concurs with the transition process from El Niño to La Nina corresponding to the seasonally evolving SST patterns (Fig.5a). Following a low-frequency El Niño event, the positive SST anomalies weaken in the central-eastern equatorial Pacific, while a basin-wide warming over the tropical Indian Ocean peaks in the subsequent spring season MAM(0). The process takes place and develops during the developing and mature phase of the low-frequency El Niño (MAM(−1) to D(−1)JF(0)). The positive H200 anomalies occupy the entire equatorial belt while SST anomalies are positive in tropical oceans in the subsequent spring season MAM(0) (Fig.5a).

In the El Niño decaying summer JJA(0), cool SSTA occurs in the central-eastern equatorial Pacific, while warm SST anomalies weaken in magnitude but remain positive over most of the Indian Ocean except off the Somali coast where the southwest monsoon strengthens over the Arabian Sea (Fig.5b). Instead of being zonally uniform, summer positive H200 anomalies are highly asymmetric in the east-west direction. High positive H200 anomalies, trapped on the equator to the east over the Maritime Continent (Fig.5a), occupy the subtropics on either side of the equator west of 70°E, indicating the Rossby and Kelvin wave responses (Gill, 1980) to a tropical heating centered on the equator. Meanwhile, the easterly wind anomalies associated with the central-eastern equatorial Pacific cooling generate an anticyclone over the Philippine Sea. This result is consistent with the capacitor mechanism that extends El Niño's impact on EAM through the IO warming (Yang *et al.*, 2007).

An early study by Yang *et al.*(2007) shows the persis-

tent IOBM influence on the Asian summer monsoon, which is characterized by a Matsuno-Gill pattern in the-upper troposphere and a low level anticyclonic pattern over the subtropical northwest Pacific (see Yang *et al.*, 2007, Figs.2 and 4). The southerly anomalies on the northwest flank of this anomalous anticyclone increase the moisture transport onto central China (Chang *et al.*, 2000a), and lead to abundant rainfall over the middle and

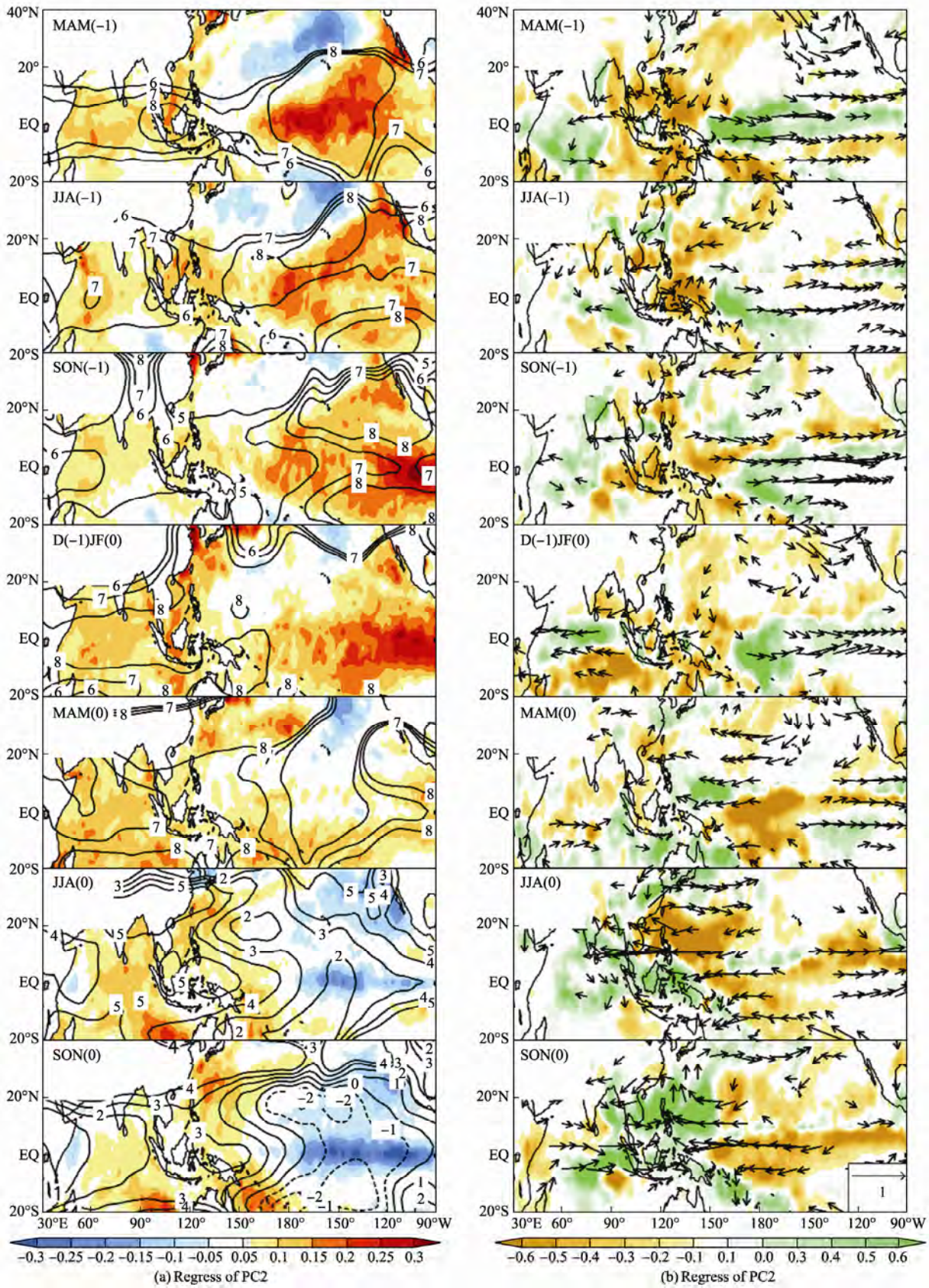

Fig.5 Seasonally evolving patterns of (a) 200 hPa geopotential height (contours in m) and SST (shaded; ℃) anomalies regressed onto PC2; (b) the same as in (a), but for 850-hPa wind ($m\,s^{-1}$; vector) and precipitation rate (shaded, $mm\,d^{-1}$).

lower reaches of the Yangtze River and Huaihe River valleys (Fig.5b). Meanwhile, the anomalous anticyclone causes dry conditions over South China, SCS and WNP, and the precipitation anomaly in summer exhibits a 'Northern Flood and Southern Drought' pattern over the east of China (Fig.2b). Therefore, besides the ENSO event the IOBM is an important factor to influence the drought/flood pattern in the rainy season over the east of China. The suppressed convection associated with this anomalous anticyclone may cause clouds to decrease and lead to the warmer SSTA in the SCS and WNP (Fig.5a).

In SON(0), the anomalous anticyclone shifts eastward associated with the development of La Nina episode (Fig.5b). The local positive SSTA persisting from the previous season enhances the convection, forces an anomalous cyclone over the SCS, and results in the abundant rainfall over the SCS and WNP (Fig.5b).

4.3 The Third Mode

Fig.6 shows the lead-lag correlations between PC3 and the Niño-3.4 index (solid line) and the partial lead-lag correlations between PC3 and the area-averaged SSTA without the influence of the Niño-3.4 index) over the tropical IO (10°S−10°N, 40°E−110°E) region. It can be seen that PC3 is positively correlated with the tropical IO SST anomaly from the spring of the preceding year(–1) to the winter of the following year(+1) without the winter D(–1)JF(0) and spring MAM(0) seasons included. On the other hand, PC3 has no close relationship with the Niño-3.4 index except in MAM(0) and after JJA(+1). This suggests that the third mode seems associated with the low frequency variability (Huang *et al.*, 2009) of IOBM and there is almost no relationship with ENSO.

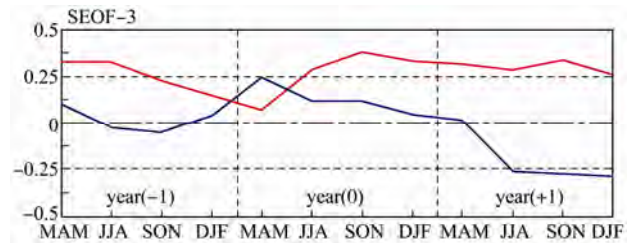

Fig.6 Lead-lag partial correlations between the third S-EOF principal component and the Niño-3.4 index (blue line), and with the Indian Ocean basin-wide warming index (red line). The Indian Ocean basin-wide warming index is defined as area-averaged SSTA in the tropical Indian Ocean (10°S−10°N, 40°E−110°E).

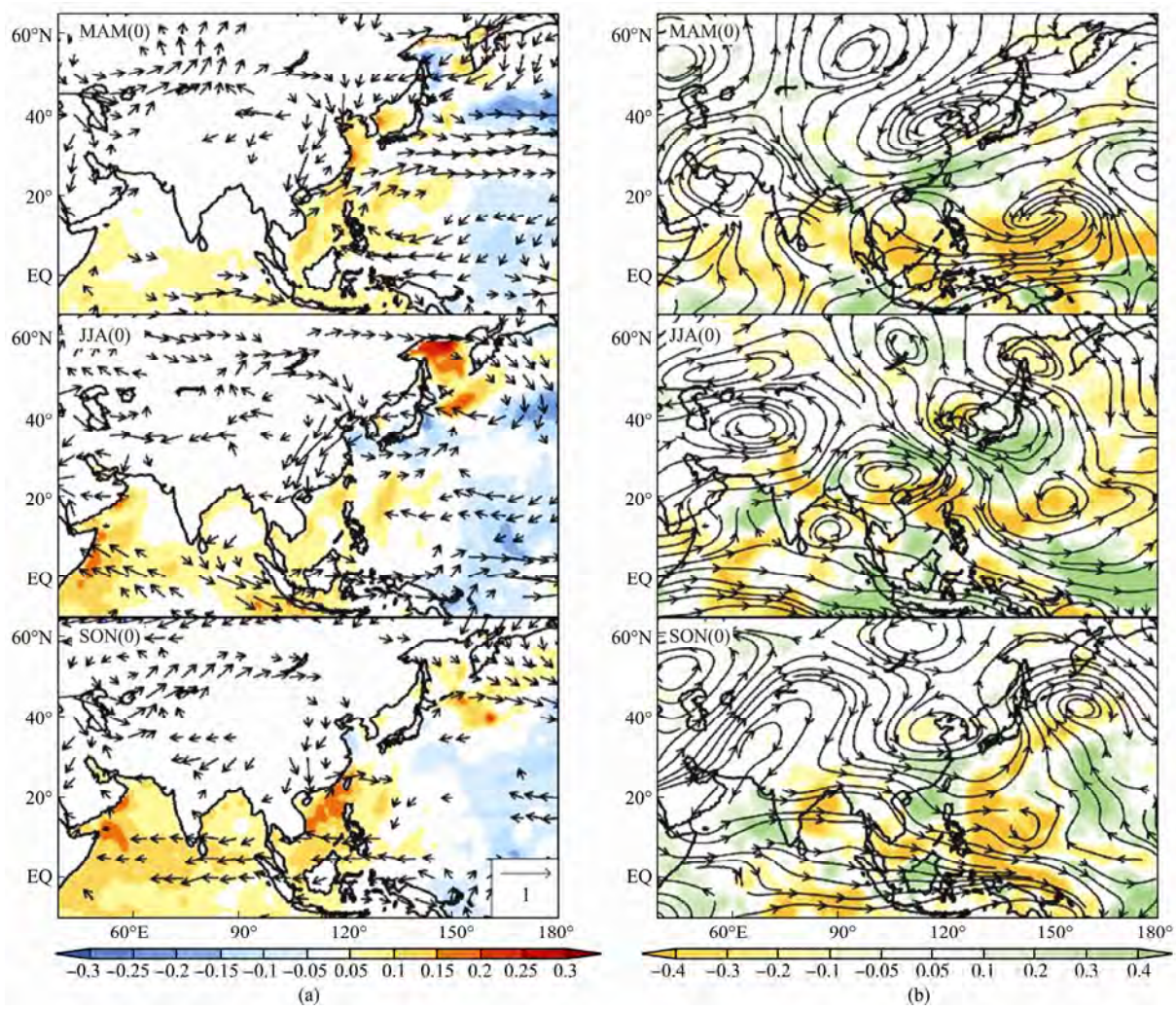

Fig.7 Seasonally evolving patterns of (a) 850-hPa wind (vector; m s^{-1}) and SST (shaded; ℃) anomalies regressed onto the principal component of the third S-EOF; (b) the same as in (a), but for precipitateion rate (shaded, mm d^{-1}) and 200-hPa streamline.

In the summer rainy season JJA(0), the regressed 850-hPa circulation shows that anomalous northerlies prevail at the mid-latitudes of East China, indicating a weak East Asian summer monsoon (Fig.7a). This feature may be associated with the warm SSTA in the SCS and the Philippine Sea throughout the rainy season. According to the definition of the index of land-sea thermal difference (ILSTD) (Sun *et al.*, 2000), this warm pattern provides favorable conditions for the weak north-south thermal contrast. The correlation between PC3 and the ILSTD from 1961−1999 is –0.72, far exceeding the 99% confidence level.

Additionally, there is an anomalous cyclone centered at 35˚N, 130˚E from South Japan to the East China Sea at the 850 hPa level in JJA(0) (Fig.7a). This anomalous cyclone has a barotropic structure with a slight northward tilt and the center at the 200 hPa level is around 40˚N, 130˚E (Fig.7b). The strong anomalous cyclone located over the East China Sea leads to abundant rainfall over the middle and lower reaches of the Yangtze River valley, the East China Sea, and southern Japan. Meanwhile, an anomalous anticyclone over southern China induces a suppressed rainfall there (Fig.7b). It is found that a wave-train-like anomalous circulation at 200 hPa extends from central Asia to the North Pacific along a path that resembles the circumglobal teleconnection route in its negative phase (Ding and Wang, 2005). The negative phase of this wave-train from central to East Asia, named as the 'Silk Road' teleconnection by Enomoto *et al.* (2003), normally occurs in August. This teleconnection and associated rainfall anomalies are similar to those in the negative phase of the non-ENSO-related JA mode (Wang *et al.*, 2009, Fig.9b). Ding and Wang (2005), and Wang *et al.* (2009) proposed that the enhanced rainfall over the northern Indian monsoon region may be linked to the north China rainfall anomalies through the 'Silk Road' teleconnection (Enomoto *et al.*, 2003) or a part of CGT (Ding and Wang, 2005). Therefore, the third mode may be related to a weak northern Indian monsoon that may occur without the ENSO impact (Ding and Wang, 2005).

Another significant feature is the persistent cold SST anomalies in the equatorial western Pacific between 150˚E and the international date line−the Niño-4 region from the spring season MAM(0) to autumn season SON(0) (Fig. 7a). This feature is similar to the negative phase of the non-ENSO related JA mode (Wang *et al.*, 2009), but how it affects the East Asian climate remains unclear.

5 Summary and Concluding Remarks

Based on the S-EOF analysis, three leading modes reveal the dominant drought/flood patterns over the east China in rainy seasons for the period of 1960−2004. The evolution of large-scale atmospheric circulation and SST patterns associated with the three leading modes is further studied.

1) The first two leading modes reflect the seasonally evolving dominant rainfall patterns during the turnabout phase of ENSO decaying years. While the first leading mode appears closely correlated with ENSO events, the third mode may not be related to ENSO events at all. On the other hand, the basin-wide IO SSTA plays a crucial role in prolonging the impact of ENSO on the second mode during the ENSO decaying summer.

2) In the decay year of El Niño, the western North Pacific (WNP) anticyclone within the tropics persists from the preceding winter to the early summer through the positive thermodynamic air-sea feedback from the local negative SSTA (Wang *et al.*, 2000). In the decaying summer of El Niño JJA(0), the WNP anticyclone, located over the Philippine Sea, transports warm and moist air toward the south of the Yangtze River, leading to wet conditions over the area (Fig.4b). As El Niño decays rapidly in spring and vanishes by summer, the IOBM warming persists through summer, unleashes its influence, and results in a Matsuno-Gill pattern in the upper troposphere. The easterly anomalies associated with the central-eastern equatorial Pacific cooling generate an anticyclone over the Philippine Sea. The southerlies on the northwest flank of this anticyclone increase the moisture transport to central China (Chang *et al.*, 2000a), and lead to abundant rainfall over the middle and lower reaches of the Yangtze River and Huaihe River valleys. The anomalous anticyclone causes dry conditions over South China and the SCS. Therefore, the precipitation anomaly in summer exhibits a meridional dipole pattern (Fig.5).

These results indicate that the rainfall over the middle and lower reaches of the Yangtze River is more abundant during the El Niño decaying summer, which is consistent with some previous studies (Huang and Wu, 1989; Liu and Ding, 1992; Shen and Lau, 1995; Weng *et al.*, 1999; Wang *et al.*, 2000). Although the first two leading modes occur during the ENSO decaying year, the drought/flood patterns in rainy seasons over the east of China are different and the relationship between ENSO and rainfall over South China and the Huaihe River valley remains elusive. In the decaying year of El Niño without the influence of IOBM, the rainfall over the Yangtze River valley and South China is more abundant, but dry conditions prevail in the Huaihe River valley. This Southern Flood and Northern Drought pattern is exhibited in the first mode (Fig.2a). On the other hand, during the El Niño decaying year, the IOBM warming persists through summer, the rainfalls over both the Yangtze River and Huaihe River valleys are abundant,, but dry conditions dominate South China. This Northern Flood and Southern Drought pattern is shown in the second mode (Fig.2b). Therefore, besides the ENSO event, IOBM is also an important factor to forecast the drought/flood pattern in the rainy season over the east of China.

3) The third mode is positively correlated with the tropical IO SST anomaly and the warm SSTA in the SCS and the Philippine Sea, but may not be related to the ENSO events. The warm SSTA in SCS and the Philippine Sea throughout the rainy season resulted from a weak north-south land-sea thermal contrast may weaken the intensity of EASM (Sun *et al.*, 2000). Meanwhile, the weakened rainfall over the northern Indian monsoon re-

gion may be linked to the third mode through the 'Silk Road' teleconnection (Enomoto *et al.*, 2003) or a part of CGT (Ding and Wang, 2005). The physical mechanisms that reveal these linkages remain elusive and invite further investigation. Additionally, further study is needed to investigate how the persistent cold SST anomalies in the western equatorial Pacific affects East Asia.

Remote forcings from the central-eastern equatorial Pacific and the tropical IO operate either separately or jointly, and have impact on the rainfall variability over East China during the different phases of ENSO. Therefore, the relationship between the East Asian rainfall and the tropical SSTA is complex. In the future it is also necessary to explore the possible role of the change in mid-latitude mean atmospheric circulation in modulating this relationship, because the East Asian monsoon is a subtropical monsoon that involves both the tropical and mid-latitude systems. In addition, the snow cover of the Tibetan Plateau and Eurasia may be associated with the East Asian summer monsoon rainfall (*e.g.*, Hsu and Liu 2003; Wu and Kirtman, 2007).

Acknowledgements

We would like to thank Prof. Bin Wang from University of Hawaii for his constructive suggestions. The work was supported by the National Basic Research Program of China (973 Program) (No. 2012CB955604), the National Natural Science Foundation of China (Nos. 40975038, 40830106), the CMA Program (GYHY200906008), and the 111 Project (B07036).

References

Chang, C. P., Zhang, Y. S., and Li, T., 2000a. Interannual and interdecadal variations of the East Asian summer monsoon and tropical Pacific SSTs. Part I: Roles of the subtropical ridge. *Journal of Climate*, **13**: 4310-4325.

Chang, C. P., Zhang, Y. S., and Li, T., 2000b. Interannual and interdecadal variations of the East Asian summer monsoon and tropical Pacific SSTs. Part II: Meridional structure of the monsoon. *Journal of Climate*, **13**: 4326-4340.

Chen, L.-T., Zong, H.-F., and Zhang, Q.-Y., 2007. The dominant modes of intraseasonal variability of summer monsoon rain belt over eastern China. *Chinese Journal of Atmospheric Sciences*, **31** (6): 1212-1222 (in Chinese with English abstract).

Deng, A. J., Tao, S. Y., and Chen, L. T., 1989. EOF analysis of China summer rainfall. *Scientia Atmospherica Sinica*. **13** (3): 289-295

Ding, Q., and Wang, B., 2005. Circumglobal teleconnection in the Northern Hemisphere summer. *Journal of Climate*, **18**: 3483-3505.

Ding, Y. H., 1992. Summer monsoon rainfall in China. *Journal of Meteorological Society of Japan*, **70**: 373-396.

Du, Y., Zhang, Y. C., and Xie, Z. Q., 2009. Location variation of the East Asia subtropical westerly jet and its effect on the summer precipitation anomaly over eastern China. *Chinese Journal of Atmospheric Sciences*, **33** (3): 581-592 (in Chinese with English abstract).

Enomoto, T., Hoskins, B. J., and Matsuda, Y., 2003. The formation mechanism of the Bonin high in August. *Quarterly Journal of the Royal Meteorological Society*, **129**: 157-178.

Gill, A. E., 1980. Some simple solutions for heat-induced tropical circulation. *Quarterly Journal of the Royal Meteorological Society*, **106**: 447-462.

Hsu, H.-H., and Liu, X., 2003. Relationship between the Tibetan Plateau heating and East Asian summer monsoon rainfall. *Geophysical Research Letters*, **30**, 2066. DOI: 10.1029/2003 GL017909.

Huang, F., Xie, R., and Huang, S., 2010. Joint modes of the Pacific-Indian Ocean sea surface temperature anomaly at interannual timescale. *Periodical of Ocean University of China*, **40** (1): 1-9 (in Chinese with English abstract).

Huang, R., and Wu, Y., 1989. The influence of ENSO on the summer climate change in China and its mechanism. *Advances in Atmospheric Sciences*, **6**: 21-32.

Huang, S. N., Huang, F., and Huang, J., 2009. The spatial and temporal variation of seasonal evolution of dominant drought/flood patterns in rainy season over China. *Periodical of Ocean University of China*, **39** (6): 1158-1164 (in Chinese with English abstract).

Kalnay, E., Kanamitsu, M., Kistler, R., Collins, W., Deaven, D., Gandin, L., Iredell, M., Saha, S., White, G., Woollen, J., Zhu, Y., Chelliah, M., Ebisuzaki, W., Higgins, W., Janowiak, J., Mo, K. C., Ropelewski, C., Wang, J., Leetmaa, A., Reynolds, R., Jenne, R., and Joseph, D., 1996. The NCEP/NCAR 40-Year reanalysis project. *Bulletin of the American Meteorological Society*, **77**: 437-471.

Kuang, X. Y., and Zhang, Y., 2006. The impacts of position abnormalities of the East Asia subtropical westerly jet on summer precipitation in the middle and lower reaches of the Yangtze River. *Plateau Meteorology*, **25** (3): 382-389 (in Chinese with English abstract).

Lau, K.-M., and Weng, H., 2001. Coherent modes of global SST and summer rainfall over China: An assessment of the regional impacts of the 1997–98 El Niño. *Journal of Climate*, **14**: 1294-1308.

Liu, Y., and Ding, Y. H., 1992. Influence of El Niño on weather and climate in China. *Acta Meteorologica Sinica*, **6**: 117-131.

Matsumoto, J. 1997. Seasonal transition of summer rainy season over Indo-China and adjacent monsoon region. *Advances in Atmospheric Sciences*. **14**: 231-245

Shen, S., and Lau, K. M., 1995. Biennial oscillation associated with the East Asian monsoon and tropical sea surface temperatures. *Journal of Meteorological Society of Japan*, **73**: 105-124.

Sun, X. R., Chen, L. X., and He, J. H., 2002. Index of land-sea thermal difference and its relation to interannual variation of summer circulation and rainfall over East Asian. *Acta Meteorological Sinica*, **60** (2): 164-172 (in Chinese).

Sun, X. R., He, J. H., and Chen, L. X., 2000. Relationship between index of land-sea thermal difference and summer rainfall in China. *Journal of Nanjing Institute of Meteorology*, **23** (3): 378-384 (in Chinese).

Tanaka, M., 1992. Intraseasonal oscillation and the onset and retreat dares of the summer monsoon over east, southeast Asia and the western Pacific region using GMS high cloud amount data. *Journal of Meteorological Society of Japan*, **70**: 613-629.

Tao, S. Y., and Chen, L. X., 1987. A review of recent research on the East Asian summer monsoon in China. In: *Monsoon Meteorology*. Chang, P. C., and Krishmurti, T. N., eds., Oxford University Press, London, 60-92.

Wan, R. J., and Wu, G. X., 2008. Temporal and spatial distribution of the spring persistent rains over southeastern china.

Acta Meteorologica Sinica, **66** (3): 310-319 (in Chinese with English abstract).

Wang, B., and An, S.-I., 2005. A method for detecting season-dependent modes of climate variability: S-EOF analysis. *Geophysical Research Letters*, **32**, L15710. DOI: 10.1029/2005GL022709.

Wang, B., Liu, J., Yang, J., Zhou, T. J., and Wu, Z. W., 2009. Distinct principal modes of early and late summer rainfall anomalies in East Asia. *Journal of Climate*, **22**: 3864-3875.

Wang, B., Wu, R. G., and Fu, X. H., 2000. Pacific-East Asian teleconnection: How does ENSO affect East Asian climate? *Journal of Climate*, **13**: 1517-1536.

Wang, B., Wu, R. G., and Li, T., 2003. Atmosphere-warm ocean interaction and its impacts on Asian-Australian monsoon variation. *Journal of Climate*, **16**: 1195-1211.

Wang, S. W., Ye, J. L., Gong, D. Y., and Chen, Z. H., 1998. Study on the patterns of summer rainfall in Eastern China. *Quarterly Journal of Applied Meteorology*, **9** (suppl.): 65-74 (in Chinese with English abstract).

Wang, X. C., and Wu, G. X., 1996. Regional characteristics of summer precipitation anomalies over China identified in a spatial uniform network. *Acta Meteorologica Sinica*, **54** (3): 324-332 (in Chinese).

Wang, X. L., and Tu, Q. P., 2002. Spatial and temporal characteristics of Dekad Precipitation in China. *Journal of Nanjing Institute of Meteorology*, **25** (5): 664-670 (in Chinese).

Wang, Z. Y., and Ding, Y. H., 2007. Climatology of rainy seasons in China. *Chinese Journal of Atmospheric Sciences*, **32**: 1-13 (in Chinese with English abstract).

Wei, F. Y., and Li, X. D., 1995. A CEOF analysis on distribution and interannual variation of drought and flood in China during the last 100 years. *Quarterly Journal of Applied Meteorology*, **6** (4): 454-460 (in Chinese).

Weng, H., Lau, K.-M., and Xue, Y., 1999. Multi-scale summer rainfall variability over China and its long-term link to global sea surface temperature variability. *Journal of Meteorological Society of Japan*, **77**: 845-857.

Wu, B., Li, T., and Zhou, T. J., 2010. Relative contributions of the Indian Ocean and local SST anomalies to the maintenance of the western North Pacific anomalous anticyclone during El Niño decaying summer. *Journal of Climate*, 23: 2974-2986.

Wu, B., Zhou, T. J., and Li, T., 2009. Seasonally evolving dominant interannual variability modes of East Asian climate. *Journal of Climate*, **22**: 2992-3005.

Wu, R., and Kirtman, B. P., 2007. Observed relationship of spring and summer East Asian rainfall with winter and spring Eurasian snow. *Journal of Climate*, **20**: 1285-1304.

Wu, Z., He, J., Li, J., and Jiang, H., 2006. The summer drought-flood coexistence in the middle and lower reaches of the Yangtze River and analysis of its air-sea background feathers in anomalous years. *Chinese Journal of Atmospheric Sciences*, **30** (4): 570-577.

Wu, Z., Li, J., He, J., Jang, Z. H., and Zhu, X. Y., 2007. Statistical climatological characteristics of drought-flood coexistence and drought-flooding flashback in Southern China during summer normal monsoon year. *Progress in Natural Science*, **17** (12): 1665-1671.

Yang, J., Liu, Q., Xie, S.-P., Liu, Z., and Wu, L., 2007. Impact of the Indian Ocean SST basin mode on the Asian summer monsoon, *Geophysical Research Letters*, **34**, L02708. DOI: 10.1029/2006GL028571.

Yang, L. M., and Zhang, Q. Y., 2007a. Anomalous perturbation kinetic energy of Rossby wave along east Asian westerly jet and its association with summer rainfall in China. *Chinese Journal of Atmospheric Sciences*, **31** (4): 586-595.

Yang, L. M., and Zhang, Q. Y., 2007b. Relationships between perturbation kinetic energy anomaly along east Asian waesterly jet and subtropical high in summer. *Journal of Applied Meteorological Science*, **18** (4): 452-459.

Zhang, Q., Liu, P., and Wu, G. X., 2003. The relationship between t he flood and drought over the lower reach of t he Yangtze River valley and the SST over the Indian Ocean and the South China Sea. *Chinese Journal of Atmospheric Sciences*, **27** (6): 992-1006.

Zhao, H. G., 1994. The rainy season in North China. *The Meteorology*, **20**: 3-8 (in Chinese).

Zhao, Z. G., 1999. *Summer Drought and Flood in China and Environmental Field*. China Meteorological Press, Beijing, 297pp (in Chinese).

Zhou, T. J., and Yu, R. C., 2005. Atmospheric water vapor transport associated with typical anomalous summer rainfall patterns in China. *Journal of Geophysical Research*, **110**, D08104. DOI: 10.1029/2004JD005413.

Zhou, T. J., Wu, B., and Wang, B., 2009. How well do Atmospheric General Circulation Models capture the leading modes of the interannual variability of Asian-Australian Monsoon? *Journal of Climate*, **22**: 1159-1173

Zhu, Q. G., Lin, J. R., and Shou, S. W., 1981. *Senior Synoptic*. Meteorological Press, Beijing, 535pp (in Chinese).

(Edited by Xie Jun)